Insights on the atomistic origin of X and W photoluminescence lines in *c*-Si from *ab initio* simulations

Iván Santos*, María Aboy, Pedro López, Luis A. Marqués, Lourdes Pelaz

Departamento de Electricidad y Electrónica, Universidad de Valladolid, E.T.S.I. de Telecomunicación, Paseo Belén 15, 47011 Valladolid, Spain

E-mail: * ivasan@tel.uva.es

Abstract. We have used atomistic simulations to identify and characterize interstitial defect cluster configurations candidates to W and X photoluminescence centers in crystalline Si. The configurational landscape of small self-interstitial defect clusters has been explored through nanosecond annealing and implantation recoil simulations using classical molecular dynamics. Among the large collection of defect configurations obtained, we have selected those defects with the trigonal symmetry of the W center, and the tetrahedral and tetragonal symmetry of the X center. These defect configurations have been characterized using *ab initio* simulations in terms of their donor levels, their local vibrational modes, the defect induced modifications of the electronic band structure, and the transition amplitudes at band edges. We have found that the so called I_3-V is the most likely candidate for W PL center. It has a donor level and local vibrational modes in better agreement with experiments, a lower formation energy, and stronger transition amplitudes than the so called I_3-I, which was previously proposed as W center. With respect to defect candidates to X PL center, our calculations have shown that none of analyzed defect candidates match all of the experimental characteristics of the X center. Although the Arai tetra-interstitial configuration previously proposed as X center cannot be excluded, the other defect candidates to X center found, I_3-C and I_3-X, cannot either being discarded.

PACS numbers: 78.55.Ap,61.82.Fk,71.55.Cn,31.15.es

Keywords: photoluminescence, crystalline silicon, irradiation defect clusters, *ab initio* calculations

Submitted to: *J. Phys. D: Appl. Phys.*

1. Introduction

The photoluminescence (PL) spectrum of crystalline Si (c-Si) shows sharp peaks at energies below the semiconductor energy gap due to radiative recombinations [1]. These PL lines open the possibility for developing silicon-based optoelectronic devices, as some authors have investigated [2]. Many PL lines have been related to particular defect configurations involving dopants or impurities [1]. Nevertheless, there are some PL lines in c-Si whose origin at the atomic level is not clear yet. The identification of the particular defects that originate PL lines is important to turn PL into a non-destructive characterization technique for defect identification [3], and to explore the nature of these radiative defects, which is interesting from a technological point of view.

The present work is focused in two intense zero-phonon lines that appear in the PL spectra of damaged c-Si, the W (1.018 eV) and X (1.040 eV) lines [4]. The centers responsible for these lines are present in ion-implanted [5, 6, 7, 8, 9] as well as in high energy electron- and proton-irradiated c-Si [10, 11]. As W and X centers are generated during irradiation processes, they coexists with a large variety of defects which makes their identification through experiments difficult. Nevertheless, experiments have provided some essential information of the W and X centers at the atomic level.

Photoluminescence measurements indicate that the W line intensity is maximized after annealing in the range $250 - 300$°C and vanishes upon annealing at ~ 500°C [5, 6]. As the W line intensity diminishes in PL spectra, the X line raises and reaches maximum intensity after annealing in the range $400-500$°C and vanishes upon annealing at ~ 600°C [5, 6, 8]. The temperature regime at which their presence is maximized along with the fact that their intensity decreases as the damage concentration increases suggest that defects responsible for these lines should be of small size [7, 8]. It is widely accepted that the W and X centers are of interstitial nature since their intensity is modified when there are self-interstitial traps (B, C) [5, 9] whereas it is practically unaffected by the presence of vacancy traps (O) [9]. From the dependence of the W photon energy under uniaxial-stress and magnetic field perturbations Davies *et al.* deduced that the W center had trigonal symmetry, and they observed a sharp local vibrational mode (LVM) at 70 meV, along with other sharp resonances at 60, 56 and 51 meV [4]. They also found that the X center could have tetrahedral or tetragonal symmetry [12]. Hayana *et al.* observed three weak peaks in the PL spectra of implanted c-Si with energies of 69.0, 67.9 and 66.2 meV that were associated to LVMs of the X center [13].

Different studies using *ab initio* simulations tried to associate interstitial defect clusters with W and X PL lines of c-Si [14, 15, 16], but they showed contradictory results. Carvalho *et al.* analyzed two tri-interstitial Si clusters as candidates for W PL center, the so called I_3-I and I_3-V [14]. They concluded that the W PL line was due to I_3-I as I_3-V did not introduce electronic states in the semiconductor gap. In contrast, Lopez *et al.* did not find enough evidences to associate I_3-I to the W line due to its high formation energy and the bad agreement of its donor level with the photon energy of the W line [15, 16]. With respect to the X line, Carvalho *et al.* suggested the tetra-

interstitial Si cluster configuration proposed by Arai *et al.* as X PL center, despite that its donor level did not agree with experimental values, and there were some discrepancies of the calculated LVMs with experiments [17]. Thus, the atomistic configurations of the W and X PL centers in *c*-Si remain unclear [18].

In this work we try to investigate the particular defects that originate the W and X lines in *c*-Si by systematically using atomistic simulations. Rather than assuming particular atomic configurations for the defect candidates to PL centers, we have used classical molecular dynamics to explore the configurational landscape of small interstitial defect clusters. Among the vast amount of defect configurations obtained, we have selected those having the symmetry of the W and X PL centers. We have characterized selected defects using *ab initio* simulations to obtain information that can be related with experimental facts, and we have discussed the suitability of defects for being PL centers from the combined analysis of the outcome of *ab initio* simulations.

2. Simulation details

Although different defects candidates have been previously proposed for W and X PL centers in *c*-Si, we have decided to make no assumptions on defect configurations of PL centers and to systematically explore possible defect candidates. We have used kinetic Monte Carlo simulations to estimate the relevant sizes of interstitial clusters that are present in *c*-Si in the ranges of implant energies and doses and annealing temperatures at which W and X PL lines are observed. Details of these simulations can be found in reference [19]. These simulations have indicated that $\sim 98\%$ of existing interstitial clusters have 5 or less interstitials for the conditions at which the intensities of W and X lines are optimized.

We have used LAMMPS code [20] to perform classical Molecular Dynamics (CMD) simulations for exploring the configurational landscape of $I_{n\leq 5}$ interstitial defect clusters from atom dynamics during annealing simulations. We have used the Tersoff empirical potential within its third parametrization to describe the Si-Si interactions [21]. Simulations have been performed at a constant temperature of 1200 K during 25 ns, and the simulation time step was 0.5 fs. The simulation cell had a lateral dimension of 6 a_0 (being a_0 the lattice parameter of *c*-Si) and contained $1728 + n$ atoms, being $n = 1, \ldots 5$ the excess of Si interstitials. Periodic boundary conditions have been applied in the three spatial directions. A large variety of defect configurations (over 100) have been extracted during the evolution of atomic positions in the annealing simulations. We have obtained their symmetry using the software FINDSYM within the ISOTROPY Software Suite [22]. Among all of the found defect configurations, we have selected those having the trigonal symmetry of the W center, and the tetragonal and tetrahedral symmetry of the X center. We have also analyzed defects generated through energetic Si recoils in order to obtain configurations from collisional events. These simulations have been also performed using LAMMPS and their particular details can be found in reference [23]. As in the case of annealing simulations, we have selected those defect

configurations having the symmetry of W and X centers.

Selected defects have been characterized using *ab initio* simulations with VASP [24, 25]. We have evaluated (i) their donor level in the gap, which can be related with the PL photon energy; (ii) the defect induced modifications of the electronic band structure, which shows whether a defect might favor or not radiative recombinations; (iii) their LVMs at the Γ point from the matrix of the second derivatives of the energy with respect to the atomic positions, which can be directly compared to the peaks that appear in the phonon-side bands of zero-phonon lines in PL spectra; and (iv) the transition amplitudes at band edges for relevant k-points from the imaginary part of the frequency dependent dielectric function within the random phase approximation, which permits evaluating which defect candidate has a stronger transition amplitude. Band structure modifications and transition amplitudes have not been considered in previous studies on the identification of PL centers in *c*-Si [14, 15, 16].

For our *ab initio* simulations we have used PBE-PAW pseudopotentials [26, 27]. Interstitial clusters I_n obtained from CMD simulations have been embedded in cubic simulation cells of *c*-Si with 216 atoms and a lattice parameter of 3×5.47 Å, which resulted in simulation cells with $216+n$ atoms. Periodic boundary conditions have been applied in the three spatial directions. We have used an energy cutoff of 550 eV and a $4 \times 4 \times 4$ Monkhorst-Pack [28] Γ-centered k-point mesh for (i), (ii) and (iii) calculations. This simulation setup results in a denser k-point mesh [14] and larger energy cutoff [15, 16] than previous studies. For (iv) calculations, we have used an energy cutoff of 150 eV and a 2x2x2 Monkhorst-Pack Γ-centered k-point mesh due to computational restrictions as we included 600 empty bands in the calculation. *Ab initio* simulations stopped when the energy difference between consecutive ionic steps in the relaxation was smaller than 10^{-4} eV/Å for (i) and (ii), 10^{-6} eV/Å for (iii), and 10^{-8} eV/Å for (iv).

3. Simulation results and discussion

3.1. Configuration selection based on symmetry

We have represented the selection of defect configurations obtained from our CMD simulations with the symmetry of the W and X centers in figure 1. For the W center, we have not directly obtained the I_3-I tri-interstitial cluster from our CMD simulations, which has been previously assigned to the W center [14]. Nevertheless, we have included it in our study for completeness. We have obtained a trigonal di-interstitial cluster configuration from recoil simulations, and the known I_3-V tri-interstitial cluster configuration from annealing simulations. The di-interstitial defect has been labeled as I_2-V since it is very similar to the I_3-V defect configuration, as it can be seen from figure 1. To the authors knowledge, this particular configuration of the Si di-interstitial cluster has not been previously identified. For the X center, all defect candidates have been obtained from the annealing simulations. We have found the so called "compact tri-interstitial" [14, 29, 30, 31, 16], I_3-C in the following, with tetrahedral symmetry.

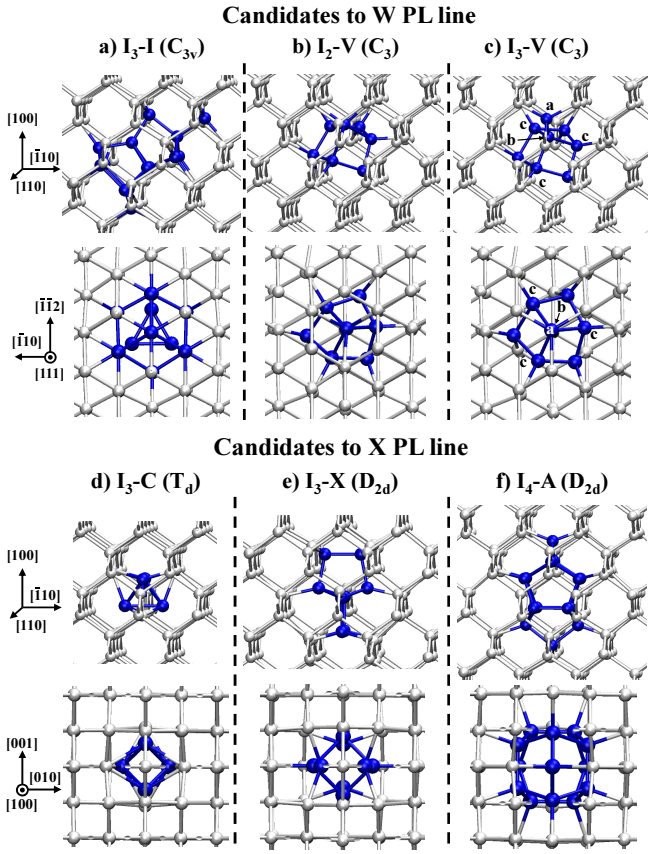

Figure 1. (Color online) Atomic configuration of found defects with the symmetry compatible with that of W and X centers. Configurations are shown on suitable projections to highlight their symmetry, which is indicated in parentheses. Silicon lattice atoms are represented by white spheres, while Si atoms belonging to defect clusters are colored in blue (dark gray).

The remaining candidates to X center found have tetragonal symmetry: a tri-interstitial defect cluster [31], I_3-X in the following, and the tetra-interstitial cluster configuration proposed by Arai, I_4-A in the following [17].

3.2. Defect formation energy and donor level

We have evaluated the formation energy of defect candidates with symmetry compatible with W and X PL centers in c-Si as

$$E_f[D^q] = E_{tot}[D^q] + E^q_{corr} - E_{tot}[bulk] - \sum_i n_i\mu_i + q[\epsilon_{VBM} + \epsilon_F] \qquad (1)$$

where $E_{tot}[D^q]$ is the total energy of the supercell with the defect in charge state q, $E_{tot}[bulk]$ is the total energy of the nondefective supercell, E^q_{corr} represents the finite size supercell charge corrections (we have applied Makov-Payne monopole charge corrections and the alignment of the electrostatic potential in the bulk-like region far from the neutral defect with respect to the bulk calculation [32]), μ_i and n_i are the chemical potential and the number of atoms added of the specie i, respectively, ϵ_{VBM} is the

Table 1. Properties of defects of figure 1 obtained from *ab initio* simulations: formation energy for neutral configurations ($E_f[D^0]$), donor levels of defects ($E_{0/+}$) obtained in this work and expected energies from PL photon energies (see text for details), and high energy LVMs at the Γ point (E_{Ph}). Parentheses in E_{Ph} energies group LVMs that imply equivalent atomic movements of the atoms belonging to the defect.

Line	**Defect**	$\mathbf{E_f[D^0]}$**(eV)**	$\mathbf{E_{0/+}}$ **(eV)**		$\mathbf{E_{Ph}}$ **(meV)**	
			This work	Expected	This work	Experiments
W	I_2-V	6.58	-	~ 0.15	61.1, 60.7, 57.9, 53.7	70, 60, 56, 51[a]
	I_3-I	7.50	0.08		74.8, 74.8, 74.5, 70.8	
	I_3-V	6.74	0.13		68.2, (59.9, 59.9)	
X	I_3-C	6.38	0.17	~ 0.13	46.2, 36.8, 34.7	69.0, 67.9, 66.2[b]
	I_3-X	6.99	0.14		62.8, 62.6, (61.6, 61.5)	
	I_4-A	7.42	0.19		63.6, (63.2, 63.2), 62.4	

[a] From reference [4].
[b] From reference [13].

Fermi energy at the valence band maximum (VBM), and ϵ_F represents the electron energy with respect to the VBM.

The formation energies of defects shown in figure 1 in the neutral charge state ($q = 0$) are summarized in table 3.2, along with other properties that will be discussed later. I_4-A is the most stable configuration of tetra-interstitial clusters found in our simulations [33]. The most stable configuration found for the Si tri-interstitial cluster is not shown in figure 1 as its symmetry is not compatible with W or X PL centers, but it agrees with the most stable I_3 configuration found in previous studies [33, 29]. The formation energies of I_3 defects shown in figure. 1 relative to the most stable configuration are 1.49 eV for the I_3-I, 0.95 eV for the I_3-X, 0.7 eV for the I_3-V, and 0.34 eV for the I_3-C. We have also found that the I_3-I has higher formation energy than the I_3-V [16], and in fact I_3-I was not obtained from our CMD simulations. I_3-X was found in previous studies as the most stable I_3 defect configuration for highly compressive biaxial strain conditions ($\epsilon \leq -2\%$), and for uniaxial strain of $\epsilon = -4\%$ has the same energy than the most stable I_3 defect configuration without strain [31]. In addition, I_3-X has the same trend in formation energy response behavior to various strain conditions as I_4-A [31].

Photon energies of zero-phonon PL lines represent energy differences between band edges and defects levels within the energy gap where carriers are recombined radiatively, or between defect levels only. In the particular case of W and X PL centers, the energy difference between band edges and the defect level should be ~ 0.15 eV and ~ 0.13 eV, respectively, according to experimental data of PL photon energies and considering an energy gap for *c*-Si close to 1.17 eV (as PL experiments are commonly performed at very low temperatures $\sim 4 - 20$ K). Defect levels are directly extracted from *ab initio* simulations through the charge transition levels of defects, which represent the Fermi energy at which the formation energy of the defect is equal in different charge states.

For example, the $E_{0/+}$ level represents the energy with respect to the VBM at which $E_f[D^{+1}] = E_f[D^0]$. Taking into account Equation (1), it is given by

$$E_{0/+} = E_{tot}[D^0] - \{E_{tot}[D^{+1}] + E^{+1}_{corr}\} - \epsilon_{VBM} \quad (2)$$

We have evaluated the charge transition levels of defects of figure 1 for $q = 0, \pm 1$. I_2-V introduces mid-gap $E_{0/+}$ donor and $E_{-/0}$ acceptor levels, which makes it incompatible with the estimation previously made on the energy difference of defect levels and band edges at studied PL centers. This is the reason why we have not reported any value associated to I_2-V in table 3.2. All remaining defects have a $E_{0/+}$ donor level, which are reported in 3.2, and none of them have a $E_{-/0}$ acceptor level within the energy gap. It can be seen from results shown in table 3.2 that I_3-V is in better agreement with the expected transition level of the W center than I_3-I, while for X center the better agreement is for I_3-X. Carvalho *et al.* did not obtained a donor level for the I_3-V and they discarded this configuration as possible W center [14].

3.3. Electronic band structure and transition amplitudes

Since PL lines are associated to radiative recombinations, the electronic band structure at defects responsible to W and X PL lines should favor direct transitions. We have represented the electronic band structure of the simulation cells containing I_3-I (figure 2.a), I_3-V (figure 2.b), I_3-C (figure 2.c), I_3-X (figure 2.d) and I_4-A (figure 2.e). It can be seen that new bands appear at the top of the valence band with respect to *c*-Si in all cases, and the bottom of the conduction band is highly modified for defects candidate to X center, being the minimum of the conduction band placed at the Γ point in the three cases.

In order to evaluate whether the observed changes in the electronic band structure might favor direct transitions between bands or not, we have calculated the amplitude for low energy direct transitions between band edges of defect candidates to W and X centers, which are represented in figure 3. Transition amplitudes of figure 3 have been extracted from the imaginary part of the dielectric function (ϵ_2) by considering those components at the energy gap region. As previously indicated, this calculation has been restricted to a $2 \times 2 \times 2$ Γ-centered k-point mesh due computational limitations. Nevertheless, this k-point mesh encompasses the Γ and X k-points, which seem to be the most relevant k-points at which direct transitions might occur as it can be seen from figure 2.

Figure 3.a shows that the amplitude of the lowest energy transition is ~ 3 times higher in I_3-V than in I_3-I, while in I_4-A it is ~ 1.3 times higher than in I_3-C, and ~ 4 times higher than in I_3-X, as it can be seen from figure 3.b. It is worth noting that the calculation of the transition amplitudes does not reveal any peak at the Γ for the I_3-X defect, as it would be expected from the band diagram of figure 2.d. Transition energies shown in figure 3 cannot be directly related to actual PL photon energies due to the underestimation of the semiconductor gap energy in DFT calculations. It would be desirable to resort to simulation techniques that overcome this limitation, such as

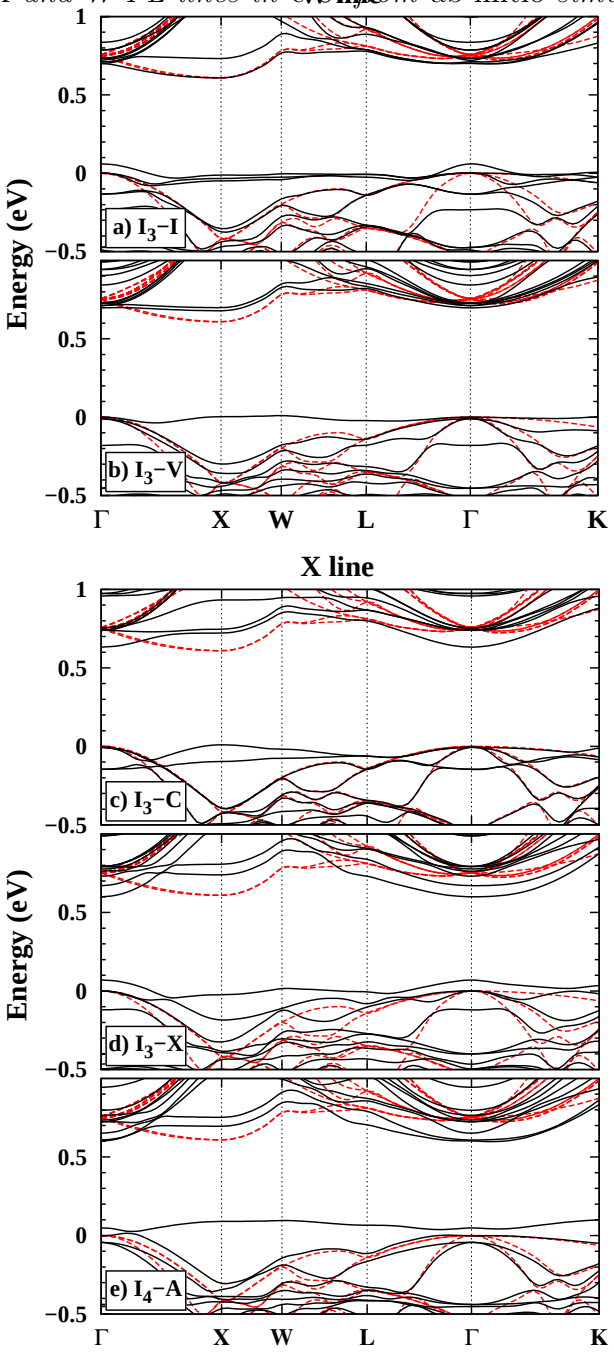

Figure 2. (Color online) Black solid lines represent the electronic band structure around the band gap region of (a) I_3-I, (b) I_3-V, (c) I_3-C, (d) I_3-X and (e) I_4-A defects in the neutral charge state. The electronic band structure of c-Si is also shown with red (gray) dashed lines. The origin of electronic energies have been placed at the top of the valence band for comparison.

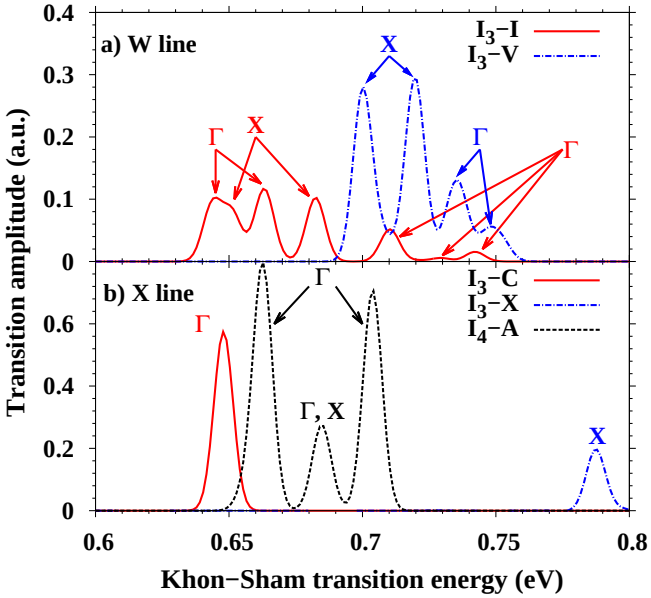

Figure 3. (Color online) Amplitudes for low energy direct transitions between band edges of defect candidates to (a) W and (b) X centers. Observed peaks correspond to transitions at indicated k-points.

GW or BSE, but the size of simulation cells considered in the present study makes it unaffordable. Nevertheless, obtained results provide very useful information for the purpose of the present study.

3.4. Local vibrational modes

Finally, we have evaluated the LVMs of defect candidates to PL centers. Obtained results are summarized in table 3.2, along with experimental measurements from literature [4, 13]. I_3-V shows a single LVM with energy slightly lower than the experimental energy, and two LVMs 8 meV below that correspond to equivalent atomic movements of the atoms belonging to the defects (indicated in parentheses in table 3.2). I_3-I has four LVMs with energies slightly above the experimental values, while LVMs of I_2-V are bellow the experimental values. Taking into account that GGA pseudopotentials tend to lower vibrational frequencies in Si [34, 35], results obtained for I_3-V are in better agreement with experiments than those of I_3-I. The high energy LVM in I_3-V corresponds to atoms a and b in figure 1.c vibrating along the C_3 symmetry axis (i.e., along its bond) with velocities in opposite directions, while c atoms vibrate in the plane perpendicular to the C_3 symmetry axis. With respect to defect candidates to X centers, LVMs of I_3-C are well bellow the experimental values, in agreement with previous calculations [15]. I_3-X and I_4-A have LVMs with similar energies, and both bellow the experimental values as it is expected from GGA pseudopotentials. In both cases there are LMVs that correspond to equivalent atomic movements that turn the 4 calculated high energy LVM into 3 as it is observed in experiments. We have evaluated the LVMs of defects in figure 1 in larger simulation cells (512+n atoms, energy cutoff

of 350 eV, and $2 \times 2 \times 2$ Monkhorst-Pack[28] Γ-centered k-point mesh), and obtained results are consistent with those obtained for the smaller simulation cell.

4. Conclusions

We have explored the vast configurational landscape of small self-interstitial defect clusters by means of CMD simulations in order to identify the defect configurations responsible for the W and X PL centers in *c*-Si. From the large collection of defect configurations obtained, we have selected those defects with the trigonal symmetry of the W center, namely I_2-V, I_3-I and I_3-V, and with the tetrahedral and tetragonal symmetry of the X center, namely I_3-C, I_3-X and I_4-A. These defects were characterized using *ab initio* simulations in order to compare the outcome of the calculations with known experimental features.

Among the defect candidates to W center, I_2-V can be discarded as it introduces donor and acceptor levels within the band gap and its LVMs are well bellow the experimental values. Although I_3-I was considered by other authors as the defect configuration responsible for the W PL line in *c*-Si, we have found that I_3-V shows a donor level and LVMs in better agreement with experiments. I_3-V has also lower formation energy, and thus its presence in the *c*-Si lattice is more probable, and it has stronger transition amplitudes than I_3-I. All this facts indicate that I_3-V is the most likely defect candidate to be associated to the W PL center in *c*-Si.

For the X center, none of analyzed defect candidates matches all of the relevant experimental features of this PL center. I_3-C shows a donor level close to the expected value and a peak for the transition amplitude at the Γ point, but its LVMs are too low in energy. I_3-X shows the best agreement of its donor level with the expected value, but carrier transitions at the Γ point seem not to be allowed as the associated peak in the transition amplitudes does not appear. A denser *k*-point mesh for the evaluation of transition amplitudes would be desirable to check whether the absence of transition amplitudes around the Γ point is consequence of the *k*-point mesh used or not, but the computational cost is unaffordable at the moment. Finally, I_4-A shows the strongest transition amplitude at the Γ among the considered defect candidates, but its donor level is higher than the expected value. LVMs of I_3-X and I_4-A are comparable, and in both cases they are slightly bellow experimental values as it is expected from GGA pseudopotentials. Our study has provided theoretical features of selected defects, but within the accuracy of our calculations, we cannot be conclusive about which one is the most likely defect candidate to X PL center in *c*-Si.

Acknowledgments

This work has been funded by the Spanish Government under project TEC2011-27701 and TEC2014-60694-P, and the JCyL Consejería de Educación y Cultura under project VA331U14. Authors thank the computational time provided by the Spanish

Supercomputing Network through project number QCM-2014-3-0034.

References

[1] Davies G 1989 *Physics Reports* **176** 83
[2] Bao J, Tabbal M, Kim T, Charnvanichborikarn S, Williams J S, Aziz M J and Capasso F 2007 *Opt. Express* **15** 6727
[3] Yoshimoto M, Okutani M, Murai G, Tagawa S, Saikusa H, Takashima S and Yoo W S 2013 *ECS J. Solid State Sci. Technol.* **2** P195–P204
[4] Davies G, Lightowlers E C and Ciechanowska Z E 1987 *J. Phys. C: Solid State Phys.* **20** 191
[5] Charnvanichborikarn S, Villis B, Johnson B, Wong-Leung J, McCallum J, Williams J and Jagadish C 2010 *Appl. Phys. Lett.* **96** 051906
[6] Johnson B C, Villis B J, Burgess J E, Stavrias N, McCallum J C, Charnvanichborikarn S, Wong-Leung J, Jagadish C and Williams J S 2012 *J. Appl. Phys.* **111** 094910
[7] Harding R E, Davies G, Hayama S, Coleman P G, Burrows C P and Wong-Leung J 2006 *Appl. Phys. Lett.* **89** 181917
[8] Harding R E, Davies G, Coleman P G, Burrows C P and Wong-Leung J 2003 *Phys. B* **738** 340
[9] Nakamura M, Nagai S, Aoki Y and Naramoto H 1998 *Appl. Phys. Lett.* **72** 1347
[10] Davies G, Hayama S, Murin L, Krause-Rehberg R, Bondarenko V, Sengupta A, Davia C and Karpenko A 2006 *Phys. Rev. B* **73** 165202
[11] Nakamura M and Nagai S 2002 *Phys. Rev. B* **66** 155204
[12] Ciechanowska Z E, Davies G and Lightowlers E C 1984 *Solid State Commun.* **49** 427
[13] Hayama S, Davies G and Itoh K M 2004 *J. Appl. Phys.* **96** 1754
[14] Carvalho A, Jones R, Coutinho J and Briddon P R 2005 *Phys. Rev. B* **72** 155208
[15] Lopez G M and Fiorentini V 2003 *J. Phys.: Condens. Matter* **15** 7851
[16] Lopez G M and Fiorentini V 2004 *Phys. Rev. B* **69** 155206
[17] Arai N, Takeda S and Kohyama M 1997 *Phys. Rev. Lett.* **78** 4265
[18] Leitão J P, Carvalho A, Coutinho J, Pereira R N, Santos N M, Ankiewicz A O, Sobolev N A, Barroso M, Lundsgaard Hansen J, Nylandsted Larsen A and Briddon P R 2011 *Phys. Rev. B* **84** 165211
[19] Aboy M, Santos I, Pelaz L, Marqus L A and López P 2014 *Journal of Computational Electronics* **13** 40–58
[20] Plimpton S 1995 *J. Comput. Phys.* **117** 1 URL `http://lammps.sandia.gov`
[21] Tersoff J 1988 *Phys. Rev. B* **38** 9902
[22] Stokes H T and Hatch D M 2005 *J. Appl. Cryst.* **38** 237 URL `http://iso.byu.edu/iso/isotropy.php`
[23] López P, Santos I, Aboy M, Marqués L A and Pelaz L 2015 *Nucl. Instrum. Meth. Phys. Res. B* **352** 156
[24] Kresse G and Furthmuller J 1996 *Comput. Mat. Sci.* **6** 15
[25] Kresse G and Furthmuller J 1996 *Phys. Rev. B* **54** 11169
[26] Perdew J P, Burke K and Ernzerhof M 1996 *Phys. Rev. Lett.* **77** 3865
[27] Kresse G and Joubert D 1999 *Phys. Rev. B* **59** 1758
[28] Monkhorst H J and Pack J D 1976 *Phys. Rev. B* **13** 5188
[29] Richie D A, Kim J, Barr S A, Hazzard K R A, Hennig R and Wilkins J W 2004 *Phys. Rev. Lett.* **92** 045501
[30] Du Y A, Hennig R G, Lenosky T J and Wilkins J W 2007 *Eur. Phys. J. B* **57** 229
[31] Bondi R J, Lee S and Hwang G S 2009 *Phys. Rev. B* **80** 125202
[32] Komsa H P, Rantala T T and Pasquarello A 2012 *Phys. Rev. B* **86** 045112
[33] Lee S and Hwang G S 2008 *Phys. Rev. B* **78** 045204
[34] Favot F and Dal Corso A 1999 *Phys. Rev. B* **60** 11427

[35] He L, Liu F, Hautier G, Oliveira M J T, Marques M A L, Vila F D, Rehr J J, Rignanese G M and Zhou A 2014 *Phys. Rev. B* **89** 064305